

# Study on Isolation Improvement Between Closely Packed Patch Antenna Arrays Based on Fractal MTM-Electromagnetic Bandgap Structures

Mohammad Alibakhshikenari <sup>1\*</sup>, Bal S. Virdee <sup>2</sup>, Chan H. See <sup>3</sup>, Raed Abd-Alhameed <sup>4</sup>, Abdul Ali <sup>1</sup>, Ammar Hussein Ali <sup>4</sup>, Francisco Falcone <sup>5</sup>, and Ernesto Limiti <sup>1</sup>

<sup>1</sup> Electronics Engineering Department, University of Rome “Tor Vergata”, Via del politecnico 00133, Rome, ITALY

<sup>2</sup> London Metropolitan University, Center for Communications Technology & Mathematics, School of Computing & Digital Media, London N7 8DB, UK

<sup>3</sup> School of Engineering Department, University of Bolton, Deane Road, Bolton, BL3 5AB, UK

<sup>4</sup> School of Electrical Engineering & Computer Science, University of Bradford, UK

<sup>5</sup> Electric and Electronic Engineering Department, Universidad Pública de Navarra, SPAIN

\* alibakhshikenari@ing.uniroma2.it

**Abstract**— A decoupling metamaterial (MTM) configuration based on fractal electromagnetic bandgap (EMBG) structure is shown to significantly enhance isolation between transmitting and receiving antenna elements in a closely packed patch antenna array. The MTM-EMBG structure is cross-shaped assembly with fractal slots etched in each arm of the cross. The fractals are composed of four interconnected ‘Y-shaped’ slots that are separated with an inverted ‘T-shaped’ slot. MTM-EMBG structure is placed between the individual patch antennas in a 2×2 antenna array. Measured results show the average inter-element isolation improvement in the complete band of interest is 17 dB, 37 dB and 17 dB between radiation elements #1 & #2, #1 & #3, and #1 & #4, respectively. With the proposed method there is no need for metallic via-holes. The proposed array covers the frequency range of 8–9.25 GHz for X-band applications, which corresponds to a fractional bandwidth of 14.5%. With the proposed method the edge-to-edge gap between the antenna can be reduced to  $0.5\lambda_0$  with no degradation in the antenna’s radiation patterns. The gain of the antenna array varies between 4 dBi and 7 dBi. The proposed method is applicable for implementation of closely packed patch antenna arrays, e.g. multiple-input-multiple-output (MIMO) systems, and synthetic aperture radars (SAR).

**Index Terms**—Fractal, mutual coupling, isolation enhancement, planar antennas, electromagnetic bandgap (EMBG), metamaterial (MTM), multiple-input-multiple-output (MIMO), synthetic aperture radar (SAR).

## I. INTRODUCTION

Electromagnetic interference between antenna elements is a major issue in multi-antenna systems. This is because mutual coupling resulting from surface currents over the antenna can seriously degrade its performance in terms of radiation gain, operating bandwidth, and radiation pattern [1]. In multi-antenna systems such as synthetic aperture radar (SAR), and multiple-input-multiple-output systems (MIMO), where multiple antennas are arranged in close-proximity causes strong mutual coupling to be generated between the antennas. The consequence of this is severe degradation in the overall antenna’s radiation efficiency which has a negative impact on channel capacity [2]. It is therefore crucial to find an effective solution that mitigates/suppresses mutual coupling in antenna arrays.

Various methods have been explored to date in the suppression of mutual coupling effects between adjacent antennas, e.g. (i) defected ground structures (DGS) [3]–[6]; (ii) neutralization-line [4], [7]; and (iii) slot combined complementary split-ring resonator. However, these

techniques degrade the radiation patterns of the antenna [8]–[10]. Other mutual coupling suppression techniques reported are based on slotted and meander line resonators but these techniques are applicable over a narrow frequency range and effect the antenna’s radiation patterns [11]–[13].

It has been demonstrated that electromagnetic bandgaps (EMBGs) structures prevent propagation of surface-waves. This property has been exploited to reduce mutual coupling in the antenna arrays [14]–[19]. It is shown in [14] an EMBG structure when located on top of a radiating layer can enhance the isolation by 10 dB. Although application of EMBG configurations in antenna arrays have been shown to improve isolation between radiating elements however as these configurations are multi-periodic that require a relatively large surface area, which is not conducive in the implementation of compact antenna arrays.

This paper provides a solution to the oversize issue encountered with antenna arrays employing conventional EMBG techniques to suppress mutual coupling between

neighbouring antennas. This is achieved with fractal-based metamaterial EMBG structures. The proposed MTM-EMBG structure is cross-shaped microstrip line with fractal slots etched in each arm of the cross. The fractal configuration is composed of four interconnected ‘Y-shaped’ slot that are separated by inverted ‘T-shape’ slots. The MTM-EMBG structure is placed between the individual patch antennas in a  $2 \times 2$  antenna array. With the proposed method the edge-to-edge gap between the antennas can be significantly reduced to  $0.5\lambda_0$  with no degradation in the antenna’s characteristics. EMBG approaches presented in [14]–[18] and [20] have edge-to-edge gap in the range of  $0.5\lambda_0$  to  $0.75\lambda_0$ . The fractal is inspired the work in [21] which is based on the 3<sup>rd</sup> iteration of Moore’s curve as a variant of Hilbert curve [22]. The proposed methodology is verified with measured results. When the antenna array is combined with the fractal decoupling **structure**, the measured results show that the average isolation is better than  $-30$  dB for  $S_{12}$ ,  $-41$  dB for  $S_{13}$ , and  $-28$  dB for  $S_{14}$  across the antenna array’s operating bandwidth of 1.25 GHz from 8 to 9.25 GHz, which is two-fold greater than reported in literature. In the above citations the antenna arrays are  $1 \times 2$  configurations whereas here we are using  $2 \times 2$  configuration. The size of the proposed antenna array is  $2.4\lambda_0 \times 3.2\lambda_0$  with edge-to-edge gap between the radiating elements of  $0.5\lambda_0$  centred at 8 GHz.

## II. FRACTAL MTM-EMBG DECOUPLING FRAME

Configuration of the reference antenna array, shown in Fig. 1(a), comprises four square patches. Each patch is excited individually through a  $50\text{-}\Omega$  waveguide port. The antenna was fabricated on FR-4 lossy substrate with thickness of 1.6 mm, dielectric constant  $\epsilon_r$  of 4.3, and loss-tangent of 0.025. The measured bandwidth of the reference antenna array, shown in Fig. 2, is 1.25 GHz from 8 to 9.25 GHz. The average mutual coupling measured between each radiation patch in this reference antenna array is  $-17.5$  dB,  $-18.5$  dB, and  $-17$  dB between radiation elements #1 & #2, #1 & #3, & #1 & #4, respectively.

To improve mutual coupling suppression between radiation elements a fractal isolator, shown in Fig. 1(b), is inserted between the patches. The fractal isolator proposed here is based on MTM-EMBG structure which is etched on each arm of a cross-shaped microstrip configuration. The fractal slots are constituted from four interconnected ‘Y-shaped’ slots that are separated with an inverted ‘T-shaped’ slot. This slot configuration was determined through investigation of numerous fractal curves. This fractal configuration was chosen as it had minimal effect on the antenna’s bandwidth and radiation characteristics. **The fractal slots behave as electromagnetic band-gap (EBG) structure that prevent propagation of certain frequency bands. Detailed explanation and analysis is given in [23],[24]. At the cutoff of the stopband, the structure works almost at its fundamental resonant frequency. It is shown here the surface current distribution density over the proposed array structure decreases dramatically with the inclusion of fractal slots. The simulation analysis reveals that with no**

**metallic patch in the middle of the array connecting the fractal structures results in unacceptable suppression in mutual coupling between the antennas #1 and #4, and between #2 and #3. This indicates the interaction between the fractal structures in the proposed technique is necessary. Also,** parameters  $a$  and  $g$  had a great influence on the mutual coupling. Maximum suppression was obtained when both these parameters had dimensions of 1 mm. The fractal isolator was inserted between the four patches as shown in Fig. 1(c).

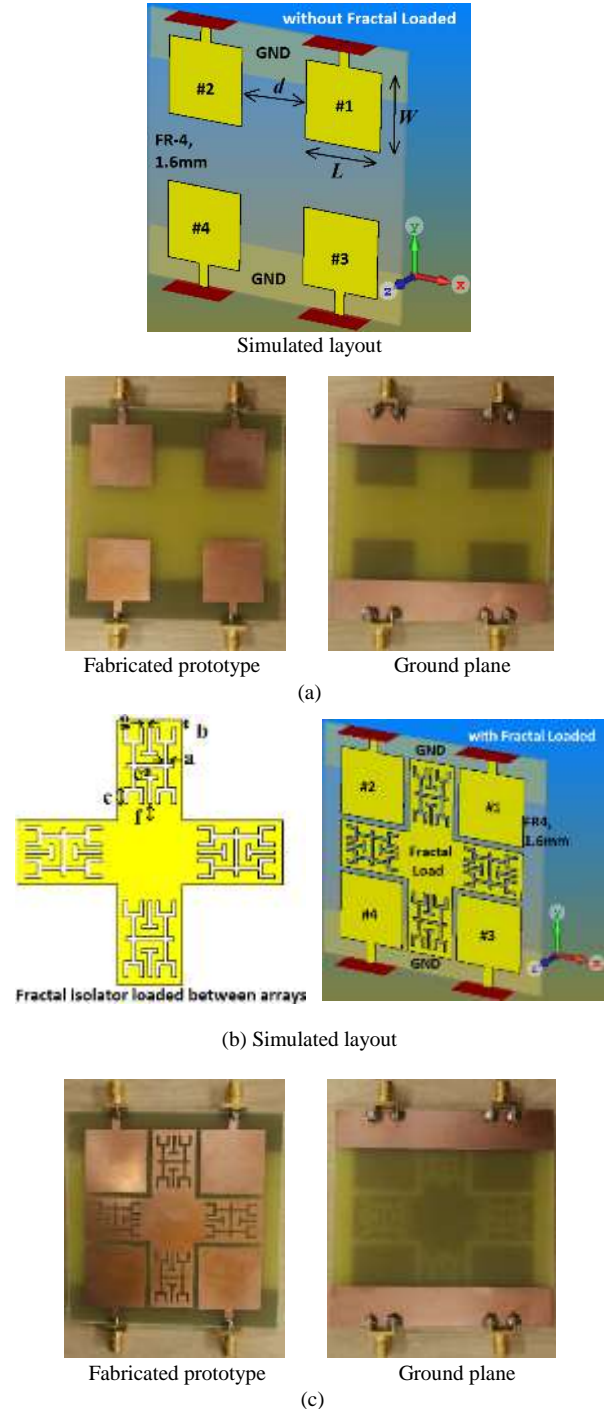


Fig.1. Layout of the antenna array, a) reference antenna array with no fractal isolator loading, b) crossed-shaped fractal decoupling **structure**, and c) antenna with fractal isolator loading.

The separation between adjacent patches is  $0.5\lambda_0$ , where  $\lambda_0$  is free-space wavelength at 8 GHz. Optimised parameters of the antenna array and fractal isolator are:  $L = 23$  mm,  $W = 23$  mm,  $a = 1$  mm,  $b = 2$  mm,  $c = 3$  mm,  $d = 20$  mm,  $e = 2$  mm,  $f = 4$  mm, and  $g = 1$  mm. **The simulated S-parameter response (Transmission and reflection coefficients) of the proposed antenna array without and with fractal MTM-EMBG isolator loading is shown in Fig. 2. It is evident that with fractal loading the isolation improvement increases from about 5 dB at 8 GHz to 18.5 dB at 9.2 GHz between antenna ports #1 and #2. However, between ports #1 and #3 the isolation degrades by about 2 dB compared with no fractal loading between 8 GHz to 8.4 GHz, but it increases between beyond 8.4 GHz up to 9.2 GHz with peak isolation improvement of about 30 dB at around 9 GHz. In the case of ports #1 and #4, isolation improvement declines from 12 dB to 8 dB from 8 GHz to about 8.9 GHz but then abruptly increases with increase in frequency with a peak improvement by about 40 dB. The disparity in mutual coupling between the antennas results from one pair used in transmit mode and the other as receive mode.**

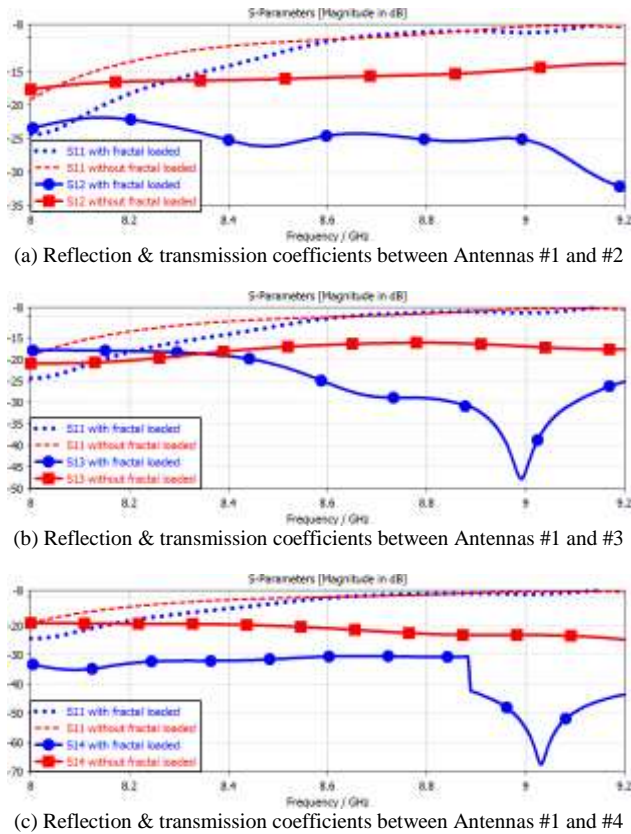


Fig. 2. Simulated reflection & transmission coefficients of the equivalent model for the proposed fractal structure.

**Fig. 3 shows the measured results of the antenna array with the proposed technique.** The antenna array with the fractal MTM-EMBG isolator has a measured bandwidth of 1.25 GHz from 8 GHz to 9.25 GHz. These results show that improvement in isolation is at the expense of reflection coefficient, however the bandwidth which is

defined for  $|S_{11}| \leq -10$  dB is the same for both cases of with and without MTM-EMBG. The average measured mutual coupling between each radiation patch with the fractal isolator are; -30 dB, -41 dB, and -28 dB between elements #1 & #2, #1 & #3, and #1 & #4 respectively. Compared with no fractal loading there is substantial improvement in mutual coupling suppression of 12.5 dB, 22.5 dB, and 11 dB between elements #1 & #2, #1 & #3, and #1 & #4 respectively. These results are given in Table I.

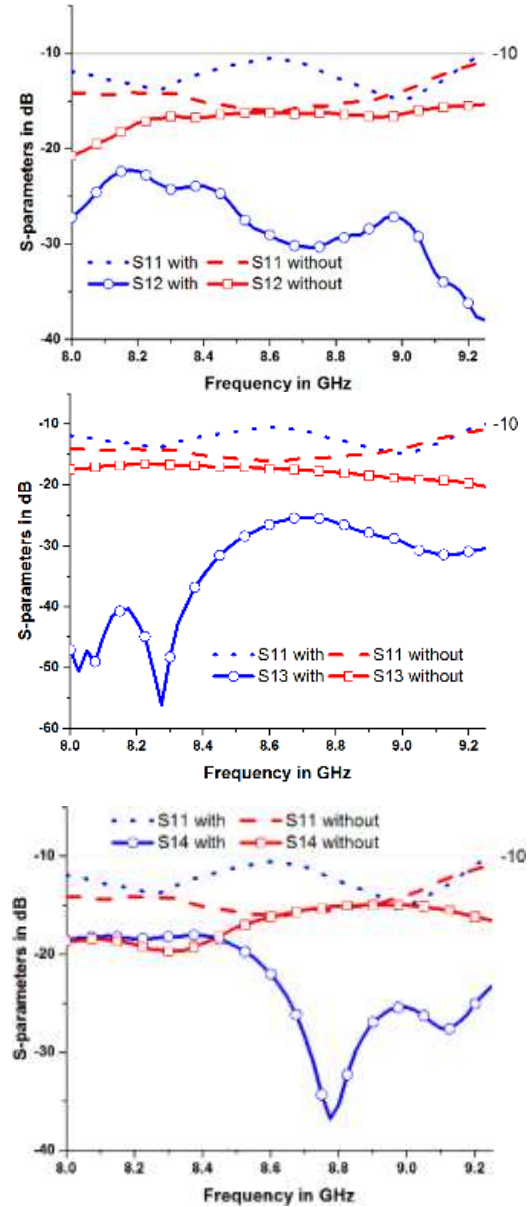


Fig. 3. Measured S-parameters with and without the fractal MTM-EMBG decoupling structure.  $S_{12}=S_{34}$ ,  $S_{13}=S_{24}$ , and  $S_{14}=S_{23}$  as the antenna array is symmetrical configuration.

The equivalent electrical circuit model of the antenna array loaded with the fractal isolator is shown in Fig. 4, where the patch radiator is represented with a resonant circuit comprising inductance  $L_P$ , capacitance  $C_P$ , and resistance  $R_P$ . Equivalent circuit of the fractal MTM-EMBG isolator is represented by inductance  $L_F$  and the capacitance  $C_F$ , whose magnitude depend on the gap between the radiators. **Metallic patch in the middle of the**

array connecting four fractal sections is modelled by inductance  $L_C$ . Coupling between patch and fractal isolator is through capacitance  $C_C$  which is more dominant because the fractal isolator is coupled to the patch via non-radiating edge of the patch antenna. Ohmic and dielectric loss associated with the fractal isolator are modelled by resistance  $R_F$ . The resonance frequency ( $f_r$ ) of the decoupling structure is dependent on the magnitude of inductance ( $L_F$ ) and capacitance ( $C_F$ ) given by:

$$f_r = \frac{1}{2\pi\sqrt{L_F C_F}} \quad (1)$$

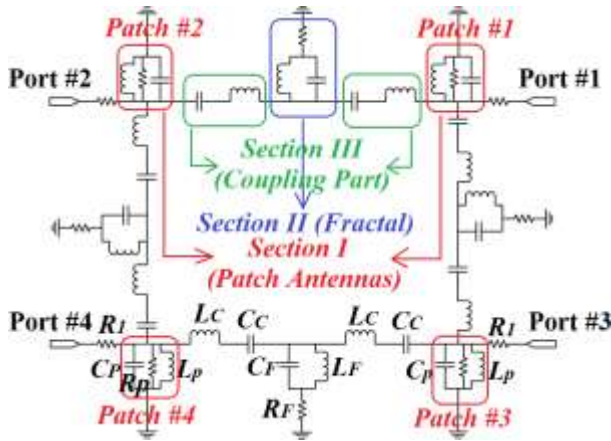


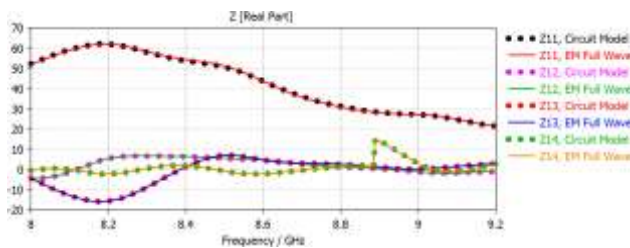
Fig. 4. Equivalent circuit diagram of the proposed antenna array.

Optimised values of the equivalent circuit model were extracted using optimization tool in full-wave EM simulation by CST over 8 GHz to 9.2 GHz. These values of these parameters are given in Table II. The simplified

TABLE II. OPTIMIZED VALUES OF THE EQUIVALENT MODEL REPRESENTING THE PROPOSED STRUCTURE

$R_P$	$C_P$	$L_P$	$C_F$	$L_F$	$R_F$	$C_C$	$L_C$	$R_I$	$R$	$L$	$C$
50 $\Omega$	1.5 pF	9.02 nH	9.7 pF	1.8 nH	75.5 $\Omega$	12.2 pF	1.0 nH	82.5 $\Omega$	~50 $\Omega$	7.5 nH	1.35 pF

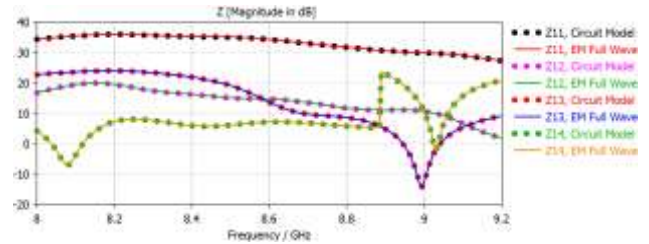
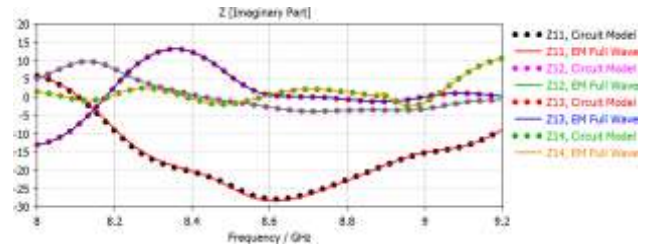
Surface current distribution without and with the fractal isolator, which is shown in Fig. 7, provide further insight on the antenna array. It is evident the cross-shaped fractal decoupling structure significantly interacts with the surface currents to block them from affecting adjacent radiation elements in the antenna array. Destructive effects of surface currents in the antenna are significantly suppressed from effecting the far-field of the antenna array.



equivalent circuit model was used to determine the effectiveness of the fractal load on the antenna array's return-loss and isolation performance. Input impedance and admittance of the proposed antenna arrays computed using full-wave EM simulation tool are shown in Figs. 5. Due to the symmetrical configuration of the antenna array and accurate estimation of the  $RLC$  parameters the circuit model and CST results are perfectly mapped on each other for both of input impedance and admittance.

TABLE I. ANTENNA ARRAY'S S-PARAMETER PERFORMANCE

$ S_{11}  \leq -10$	8.0 - 9.25 GHz (BW = 1.25 GHz, FBW = 14.5%)
$S_{12} = S_{34}$ with isolator	Max.: -38 dB @ 9.25 GHz, Min.: -22 dB @ 8.15 GHz, Ave.: -30 dB
$S_{12} = S_{34}$ without isolator	Max.: -21dB @ 8.0 GHz Min.: -15 dB @ 9.25 GHz, Ave.: -17.5 dB
Isolation improvement	Max.: 17 dB, Min.: 7 dB, Ave.: 12.5 dB
$S_{13} = S_{24}$ with isolator	Max.: -57 dB @ 8.27 GHz Min.: -25 dB @ 8.7 GHz, Ave.: -41 dB
$S_{13} = S_{24}$ without isolator	Max.: -20 dB @ 9.25 GHz Min.: -17 dB @ 8.2 GHz, Ave.: -18.5 dB
Isolation improvement	Max.: 37 dB, Min.: 8 dB, Ave.: 22.5 dB
$S_{14} = S_{23}$ with isolator	Max.: -37 dB @ 8.85 GHz Min.: -18 dB @ 8.38 GHz, Ave.: -28 dB
$S_{14} = S_{23}$ without isolator	Max.: -20 dB @ 8.3 GHz Min.: -15 dB @ 8.86 GHz, Ave.: -17 dB
Isolation improvement	Max.: 17 dB, Min.: 3 dB, Ave.: 11 dB



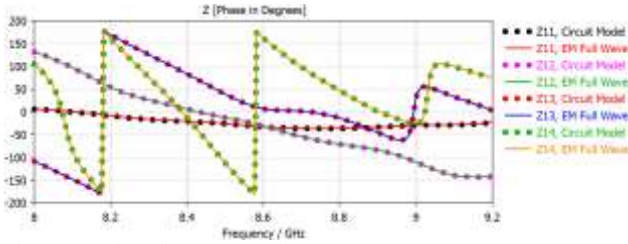


Fig. 4. Input impedances ( $\Omega$ ) of the proposed antenna arrays.

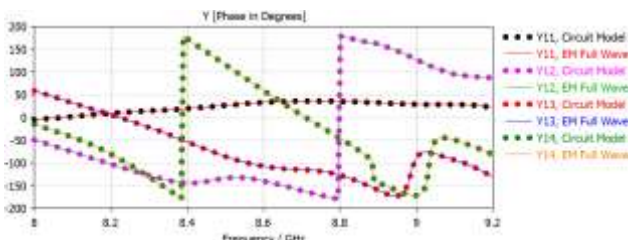
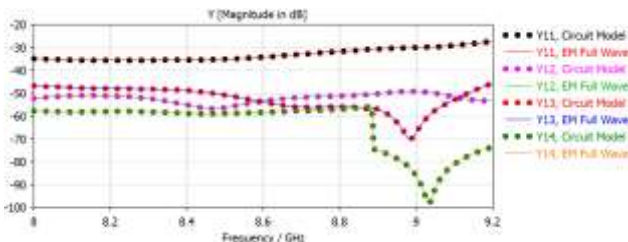
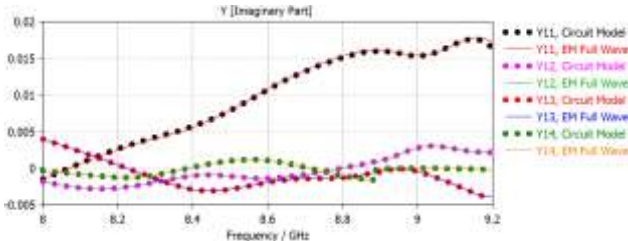
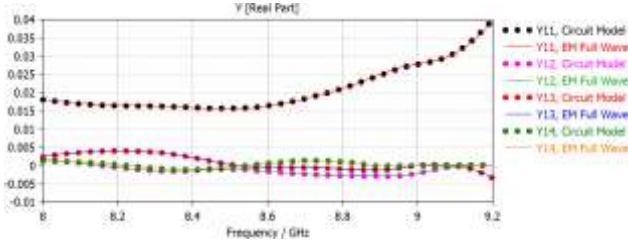
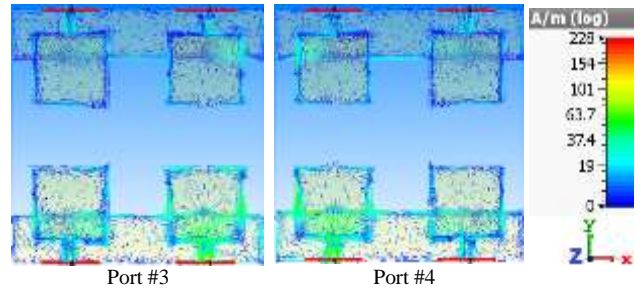
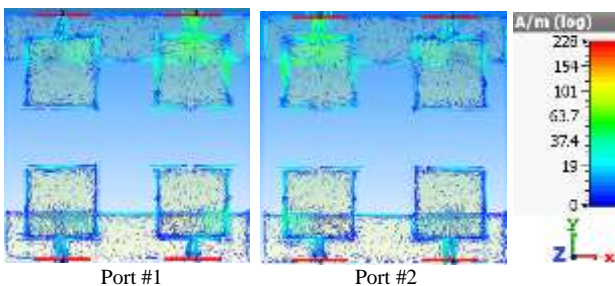
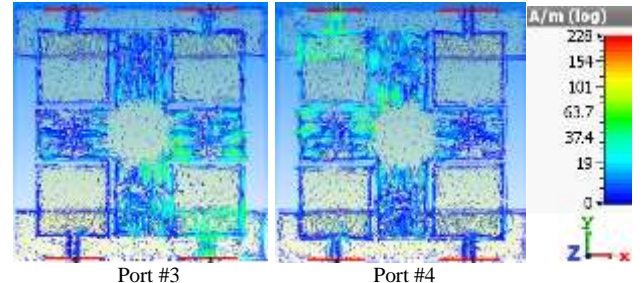
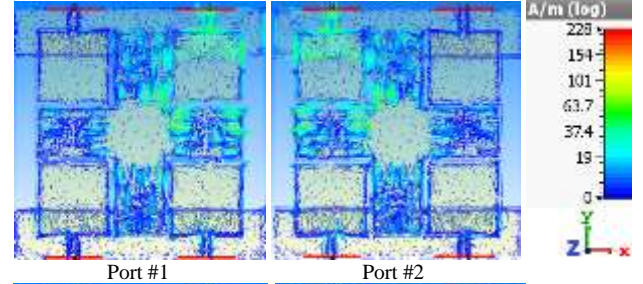


Fig. 5. Input admittances ( $1/\Omega$ ) of the proposed antenna arrays.

Radiation performance of the antenna array was measured in a spherical chamber. Fig. 7 shows the measured radiation patterns of the four patch antennas in the array with and without fractal decoupling structure. Compared to the reference antenna array, the radiation characteristics of the array with the cross-shaped fractal MTM-EMBG structure is a crude approximation.

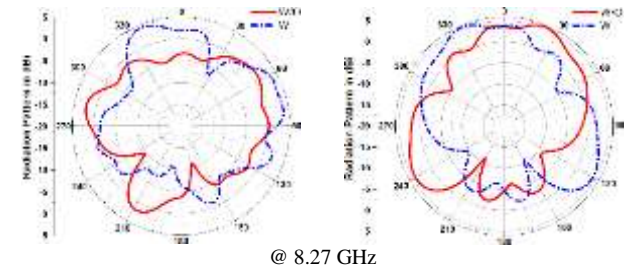


(a) No fractal loading

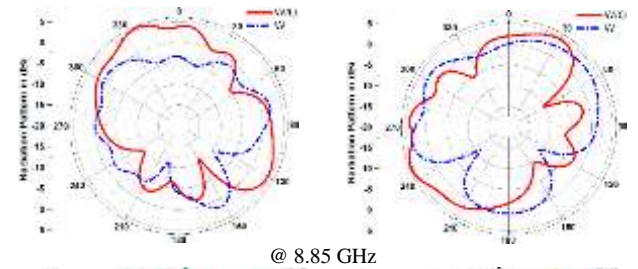


(b) Fractal loading

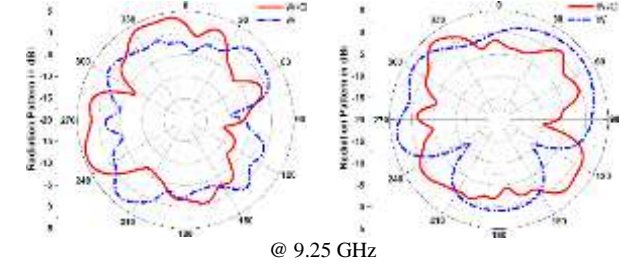
Fig. 6. Surface current density distributions over the antenna array at 8.27 GHz.



@ 8.27 GHz



@ 8.85 GHz



@ 9.25 GHz

Fig. 7. Measured radiation patterns, left and right columns represent H- and E-planes, respectively.

### III. COMPARISONS WITH OTHER ANTENNAS

The proposed antenna array is compared with the several recent works in Table III. In the literature, all the antenna designs are constructed using two radiation elements. However, in our present work, we have increased the array elements to four to give a more accurate representation. In addition, all the references cited in Table III have used the defected ground structure (DGS) technique to enhance isolation between the two radiating elements. Whereas the proposed antenna array has a truncated ground-plane to improve the impedance

bandwidth of the antenna array. **It is also evident from the table that antenna arrays with smaller edge-to-edge gap operate over a narrow bandwidth and their radiation patterns are degraded, whereas the proposed antenna array operates a wider bandwidth and its radiation patterns are unaffected.** The proposed method described here offers an optimum isolation between adjacent antennas of 37 dB, which is significantly better than isolation in other references except for [5]. However, in [5] the antenna use short-circuit vias, which is not used in our case. The proposed technique is simple to implement in practice.

TABLE III. COMPARISON OF THE PROPOSED ANTENNA ARRAY WITH RECENT WORKS (FBW is fractional bandwidth)

Ref.	Method	Max. isolation improvement	Bandwidth (FBW)	Rad. pattern deterioration	No. of elements	Edge-to-Edge Gap
[5]	Slot in Ground plane	40 dB	Narrow	Yes	2	$0.33\lambda_0$
[6]	DGS	17.4dB	Narrow	Yes	2	$0.23\lambda_0$
[9]	SCSRR	10 dB	Narrow	Yes	2	$0.25\lambda_0$
[10]	SCSSRR	14.6 dB	Narrow	Yes	2	$0.125\lambda_0$
[11]	Compact EBG	17 dB	Narrow	Yes	2	$0.8\lambda_0$
[12]	U-Shaped Resonator	10 dB	Narrow	Yes	2	$0.6\lambda_0$
[13]	Meander Line Resonator	10 dB	Narrow	No	2	$0.055\lambda_0$
[14]	UC-EBG	14 dB	Narrow	Yes	2	$0.5\lambda_0$
[15]	EBG	10 dB	Narrow	Yes	2	$0.5\lambda_0$
[16]	EBG	8.8 dB	Narrow	-	2	$0.75\lambda_0$
[17]	EBG	5 dB	Wide (~16%)	-	2	$0.6\lambda_0$
[18]	EBG	13 dB	Wide (~12%)	Yes	2	$0.5\lambda_0$
[19]	EBG&DGS	16 dB	Narrow	No	2	$0.6\lambda_0$
[20]	Fractal load with DGS	16 dB	Narrow (2.5%)	No	2	$0.22\lambda_0$
[25]	EBG	4 dB	Narrow	Yes	2	$0.84\lambda_0$
[26]	Slotted Meander-Line Resonator	16 dB	Narrow	Yes	2	$0.11\lambda_0$
[27]	I-Shaped Resonator	30dB	Narrow	Yes	2	$0.45\lambda_0$
[28]	W/g MTM	20 dB	Narrow	No	2	$0.125\lambda_0$
[29]	W/g MTM	18 dB	Narrow	No	2	$0.093\lambda_0$
<b>This work</b>	Fractal MTM-EMBG	17 dB for $S_{12}$ 37 dB for $S_{13}$ 17 dB for $S_{14}$	Wide > 1 GHz (~15%)	No	4	$0.5\lambda_0$

### IV. CONCLUSIONS

An innovative decoupling **structure** based on fractal MTM-EMBG has been presented to significantly improve isolation in antenna arrays. The proposed fractal isolator has negligible effect on the antenna array's frequency bandwidth and radiation characteristics. In addition, the proposed technique is simple to implement and does not require short-circuit vias. **The average isolation in the complete band of interest is better than 17 dB.** With the proposed technique the edge-to-edge spacing between antennas can be reduced to  $0.5\lambda_0$ , which facilitates compact designs. The proposed decoupling structures can be applied to realise closely packed patch antenna arrays for multiple-input-multiple-output (MIMO) systems and synthetic aperture radar (SAR).

### REFERENCES

[1] A. Ludwig, "Mutual coupling, gain and directivity of an array of two identical antennas," *IEEE Trans. Antennas Propag.*, vol. AP-24, no. 6, pp. 837–841, Nov. 1976.  
[2] R. Janaswamy, "Effect of element mutual coupling on the capacity of fixed length linear arrays," *IEEE Antennas Wireless Propag. Lett.*, vol. 1, pp. 157–160, 2002.

[3] A. Habashi, J. Naurinia, and C. Ghabadi, "A rectangular defected ground structure (DGS) for reduction of mutual coupling between closely-spaced microstrip antennas," *Proc. 20th Iranian Conf. Elect. Eng.*, Tehran, Iran, 2012, pp. 1347–1350.  
[4] C.M. Luo, J. S. Hong, and L. L. Zhong, "Isolation enhancement of a very compact UWB-MIMO slot antenna with two defected ground structures," *IEEE Antennas Wireless Propag. Lett.*, vol. 14, pp. 1766–1769, 2015.  
[5] OuYang, J., F. Yang, and Z. M. Wang, "Reduction of mutual coupling of closely spaced microstrip MIMO antennas for WLAN application," *IEEE Ant. Wireless Propag. Letters*, vol. 10, pp. 310–312, 2011.  
[6] Zhu, F. G., J. D. Xu, and Q. Xu, "Reduction of mutual coupling between closely packed antenna elements using defected ground structure," *Electronics Letters*, vol. 45, no. 12, pp. 601–602, 2012.  
[7] T. C. Tang and K. H. Lin, "An ultrawideband MIMO antenna with dual band-notched function," *IEEE Antennas Wireless Propag. Lett.*, vol. 13, pp. 1076–1079, 2014.  
[8] Z. Qamar, U. Naem, S. A. Khan, M. Chongcheawchanman, and M. F. Shafique, "Mutual coupling reduction for high performance densely packed patch antenna arrays on finite substrate," *IEEE Trans.*

- Antennas Propag.*, vol. 64, no. 5, pp. 1653–1660, May 2016.
- [9] Suwailam, M. M. B., O. F. Siddiqui, and O. M. Ramahi, “Mutual coupling reduction between microstrip patch antennas using slotted-complementary split-ring resonators,” *IEEE Antennas & Wireless Propag., Lett.*, vol. 9, pp. 876–878, 2010.
- [10] Shafique, M. F., Z. Qamar, L. Riaz, R. Saleem, and S. A. Khan, “Coupling suppression in densely packed microstrip arrays using metamaterial structure,” *Microwave and Optical Technology Letters*, vol. 57, No. 3, pp. 759–763, 2015.
- [11] Islam, M. T. and M. S. Alam, “Compact EBG structure for alleviating mutual coupling between patch antenna array elements,” *Progress in Electromagnetics Research*, vol. 137, pp. 425–38, 2013.
- [12] Farsi, S., D. Schreurs, and B. Nauwelaers, “Mutual coupling reduction of planar antenna by using a simple microstrip u-section,” *IEEE Antennas & Wireless Propag. Letters*, vol. 11, pp. 1501-1503, 2012.
- [13] Jeet Ghosh, Sandip Ghosal, Debasis Mitra, and Sekhar Ranjan Bhadra Chaudhuri, “Mutual Coupling Reduction between Closely Placed Microstrip Patch Antenna Using Meander Line Resonator,” *Progress in Electromagnetic Research Letters*, vol. 59, pp. 115–122, 2016.
- [14] H. S. Farahani, M. Veysi, M. Kamyab, and A. Tadjalli, “Mutual coupling reduction in patch antenna arrays using a UC-EBG superstrate,” *IEEE Antennas & Wireless Prop. Lett.*, vol. 9, pp. 57–59, 2010.
- [15] E. Rajo-Iglesias, O. Quevedo-Teruel, and L. Inclin-Sanchez, “Mutual coupling reduction in patch antenna arrays by using a planar EBG structure and a multilayer dielectric substrate,” *IEEE Trans. Antennas Propag.*, vol. 56, no. 6, pp. 1648–1655, Jun. 2008.
- [16] F. Yang and Y. Rahmat-Samii, “Microstrip antennas integrated with electromagnetic band-gap (EBG) structures: A low mutual coupling design for array applications,” *IEEE Trans. Antennas Propag.*, vol. 51, no. 10, pp. 2936–2946, Oct. 2003.
- [17] G. Exposito-Dominguez, J. M. Fernandez-Gonzalez, P. Padilla, and M. Sierra-Castaner, “New EBG solutions for mutual coupling reduction,” *Eur. Conf. Antennas Propag.*, Prague, Czech Republic, 2012, pp. 2841–2844.
- [18] M. J. Al-Hasan, T. A. Denidni, and A. R. Sebak, “Millimeter wave compact EBG structure for mutual coupling reduction applications,” *IEEE Trans. Antennas Propag.*, vol. 63, no. 2, pp. 823–828, Feb. 2015.
- [19] G. Exposito-Dominguez, J. M. Fernandez-Gonzalez, P. Padilla, and M. Sierra-Castaner, “Mutual coupling reduction using EBG in steering antennas,” *IEEE Antennas & Wireless Propag. Lett.*, vol. 11, pp. 1265–1268, 2012.
- [20] X. Yang, Y. Liu, Y.-X. Xu, and S.-X. Gong, “Isolation enhancement in patch antenna array with fractal UC-EBG structure and cross slot,” *IEEE Antennas & Wireless Propag. Lett.*, vol. 16, 2017, pp. 2175–2178.
- [21] J. Zhang, G. Ci, Y. Cao, N. Wang, and H. Tian, “A wide bandgap slot fractal UC-EBG based on Moore space-filling geometry for microwave application,” *IEEE Antennas & Wireless Propag. Lett.*, vol. 16, pp. 33–37, 2017.
- [22] J. Anguera, C. Puente, E. Martinez, and E. Rozan, “The fractal Hilbert monopole: A two-dimensional wire,” *Microw. Opt. Technol. Lett.*, vol. 36, no. 2, pp. 102–104, Jan. 2003.
- [23] J. Zhang, G. Ci, Y. Cao, N. Wang, and H. Tian, “A Wide Band-Gap Slot Fractal UC-EBG Based on Moore Space-Filling Geometry for Microwave Application,” *IEEE Antennas and Wireless Propagation Letters*, 2017, Vol. 16, pp.33-37.
- [24] B. Biswas, R. Ghatak, and D. R. Poddar, “UWB monopole antenna with multiple fractal slots for band-notch characteristic and integrated Bluetooth functionality,” *Journal of Electromagnetic Waves and Applications*, 2015, Vol. 29, Issue 12, pp. 1593-1609.
- [25] Yu, A. and X. Zhang, “A novel method to improve the performance of microstrip antenna arrays using a dumbbell EBG structure,” *IEEE Antennas & Wireless Propag. Letters*, vol. 2, No. 1, pp. 170–172, 2003.
- [26] Alsath, M. G., M. Kanagasabai, and B. Balasubramanian, “Implementation of slotted meander line resonators for isolation enhancement in microstrip patch antenna arrays,” *IEEE Antennas and Wireless Propag. Letters*, vol. 12, pp. 15–18, 2013.
- [27] Ghosh. C. K. and S. K. Parui, “Reduction of mutual coupling between E-shaped microstrip antennas by using a simple microstrip I-section,” *Microwave & Optical Tech. Lett.*, vol. 55, no. 11, pp. 2544–2549, 2013.
- [28] Yang, X. M., X. G. Liu, X. Y. Zhu, and T. J. Cui, “Reduction of mutual coupling between closely packed patch antenna using waveguide metamaterials,” *IEEE Antennas & Wireless Propag. Lett.*, vol. 11, pp. 389-391, 2012.
- [29] Qamar, Z. and H. C. Park, “Compact waveguided metamaterials for suppression of mutual coupling in microstrip array,” *Progress in Electromagnetic Research*, vol. 149, pp. 183–192, 2014.